

UNCLASSIFIED

AD 406 460

DEFENSE DOCUMENTATION CENTER

FOR

SCIENTIFIC AND TECHNICAL INFORMATION

CAMERON STATION, ALEXANDRIA, VIRGINIA



UNCLASSIFIED

NOTICE: When government or other drawings, specifications or other data are used for any purpose other than in connection with a definitely related government procurement operation, the U. S. Government thereby incurs no responsibility, nor any obligation whatsoever; and the fact that the Government may have formulated, furnished, or in any way supplied the said drawings, specifications, or other data is not to be regarded by implication or otherwise as in any manner licensing the holder or any other person or corporation, or conveying any rights or permission to manufacture, use or sell any patented invention that may in any way be related thereto.

(4) 560 (5) 1300 (7) + (8) NA  
9) Final Rept. 15 Apr 62 - 14 Apr 63,

Copy No. 136

Issue Date: (11) 28 May 1963

(14) ~~Report~~ No. 652/SA4/2/2/F-1,  
Vol. 6 #11

(12) 14. (13) NA  
16 17 18 19 NA  
20 21 22 NA

(16) DEVELOPMENT OF PERISCOPE FOR  
THRUST CHAMBER COMBUSTION ANALYSIS.

(10) By J. D. O'Donnell.

(15) Contract AF 04(647) 652/SA4

Aerojet-General Product Engineering Program

Prepared by

AEROJET-GENERAL CORPORATION  
Liquid Rocket Plant  
Sacramento 9, California

Prepared for

BALLISTIC SYSTEMS DIVISION  
AIR FORCE SYSTEMS COMMAND  
Air Force Unit Post Office  
Los Angeles 45, California

Handwritten: 11/1/63

63-1002  
0626

Report No. 652/SA4-2.2-F-1, Volume 6

**AEROJET-GENERAL CORPORATION**

FOREWORD

This is Volume 6 of the final report for work performed under the Aerojet-General Product Engineering Program. This report has been prepared in accordance with AFBM Exhibit 58-1 and is submitted in partial fulfillment of Contract AF 04(647)-652, Supplemental Agreement No. 4 and 33.

The final report has six volumes, each covering a separate project and complete within itself. An index of volumes comprising the report follows.

Direction for contract performance was provided by C. M. Beighly, Manager, and C. L. D'Ooge, Senior Project Engineer, Senior Research Department, Liquid Rocket Plant. The project engineer was J. D. O'Donnell, of the Advanced Chemical Research Department.

The developmental work on a periscope to visually investigate the combustion processes of full-scale thrust chambers is presented in this volume. This program was conducted during the contract period 15 April 1962 to 14 April 1963.

INDEX OF VOLUMES

- Volume 1 Ablative Thrust Chamber Feasibility  
F. W. Allen, Project Engineer
- Volume 2 Coated Metallic Thrust Chambers  
S. E. Adair, Project Engineer
- Volume 3 Expandable Nozzles  
D. M. Green, Project Engineer
- Volume 4 A Simple Vapor Pressurization System for a Liquid Rocket  
Engine (VāPak)  
W. J. Sprow, Project Engineer
- Volume 5 Metalized Thixotropic Propellants  
A. J. Aitken and L. E. Dean, Project Engineers
- Volume 6 Development of a Periscope for Thrust Chamber  
Combustion Analysis  
J. D. O'Donnell, Project Engineer

TABLE OF CONTENTS

	<u>PAGE NO.</u>
I. INTRODUCTION	1
A. OBJECTIVE	1
B. APPROACHES	2
C. SUMMARY	4
II. TECHNICAL EFFORT	5
A. QUARTZ DOME DEVELOPMENT	5
B. OPTICAL DESIGN	16
C. MECHANICAL DESIGN	19
D. COMPLETED EQUIPMENT	20
E. PLANS FOR FUTURE WORK	21

Report No. 652/SA4-2.2-F-1, Volume 6

AEROJET-GENERAL CORPORATION

TABLE LIST

TABLE NO.

Quartz Dome Evaluation Tests	1
Periscope Specifications	2

FIGURE LIST

<u>FIGURE NO.</u>		<u>PAGE NO.</u>
1	Thrust Chamber Periscope	2
2	Quartz Dome Test Fixture	10
3	Quartz Dome Test	12
4	Quartz Dome Test Injector	14
5	Quartz Dome Test Fixture No. 1	15
6	Quartz Dome Test Installation	17
7	Quartz Dome Test Motor	18
8	Quartz Dome Test Fixture No. 2	22
9	Injector Assembly	23
10	Detailed Design of Periscope Assembly	26
11	Periscope Assembly	30
12	Thrust Chamber Assembly	32



406 460

Report No. 652/SA4-2.2-F-1, Volume 6

AEROJET-GENERAL CORPORATION

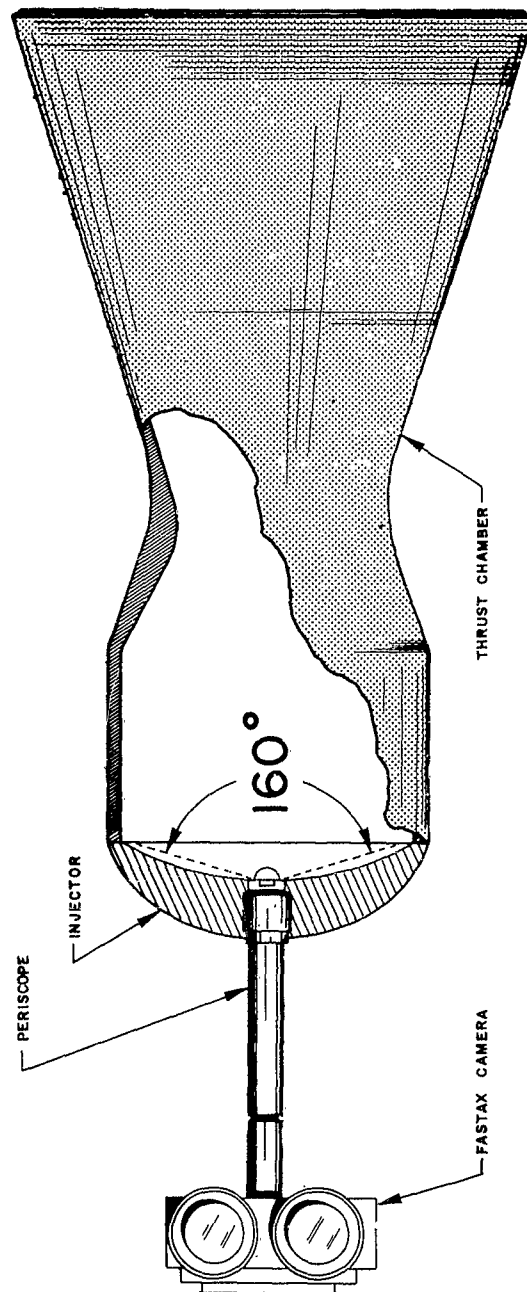
I. INTRODUCTION

A. OBJECTIVE

The object of the high-frequency combustion instability *study* portion of the Product Engineering Program was to develop a periscope to permit visual study of high-frequency instability and other phenomena of the combustion process in full-scale thrust chambers. Emphasis ~~has~~ <sup>will</sup> ~~been~~ placed on developing a reliable device to protect the optical system from the heat, erosion, and pressure of combustion, and designing a versatile optical system with a high resolution and wide field of view. The optical system, called a periscope, will be capable of being used for high-speed color photography of the combustion process. The system is designed to be used as illustrated in Figure 1.

Photography of the combustion process has been a very successful analytical technique in the past. Both pulse motors and wedge motors have been photographed through a periscope by using the inherent luminosity of the chemical reaction of the propellants to provide sufficient light for film exposure. <sup>(1)</sup>

(1) H.C. Krieg, Jr., L.O. Schulte, P.D. Gray, Liquid Thrust Chamber Development Tools, Aerojet-General Corporation, Report No. 1858, August 1960 (Confidential)



Thrust Chamber Periscope

I, A, Objective (cont.)

Although the pulse motor and wedge motor are useful for combustion analysis, they have limitations: The narrow slit window of the pulse motor cannot provide a full view of the interior of the chamber, and the configuration of the wedge motor cannot support many of the common modes of instability, such as tangential or transverse waves.

The periscope will provide a nearly complete view of the interior of an operating thrust chamber. It could be installed in either a research tool, such as a pulse motor, or in a full-scale thrust chamber assembly, such as the Titan LR91-AJ-3 or LR91-AJ-5.

B. APPROACHES

The main task in this work was to develop a device to effectively protect the optical system of the periscope from the effects of combustion. In this approach, a hemispherical dome had to be developed so that the principle light rays would enter the periscope system perpendicular to the surface of the dome, thus providing

I, B, Approaches (cont.)

full light intensity to the limits of the view field. This approach eliminates a common fault of an ordinary wide-angle lens, i.e. reflection from the first surface of the lens system.

The optical system was designed to be capable of being installed in a variety of locations in the thrust chamber and to provide the most complete view of the interior of the combustion chamber. To achieve the greatest possible field of view, commensurate with the problems involved in exposing the optics to the high temperatures of combustion, was one of the major problems to be resolved.

To achieve this, a periscope was designed with a  $160^\circ$  field of view that is passed through a 0.1-in. diameter aperture in the front surface of the housing. The design has provisions for cooling so that the periscope may be placed in a variety of locations in the thrust chamber.

I, Introduction (cont.)

C. SUMMARY

The objectives of the first year of periscope development have been completed. The objectives were: to develop and test a quartz dome capable of withstanding exposure to combustion gases at 850 psi chamber pressure, and to complete the optical and mechanical designs of the experimental periscope.

Seven tests were conducted on two quartz dome test fixtures. The first fixture, an unpolished dome, was exposed to combustion in five thrust chamber firings for a total of 6 sec at 850 psia chamber pressure. The second fixture, a polished optical-quality dome, was exposed to two thrust chamber firings for a total of 3 sec at 850 psia chamber pressure. The propellants used were  $N_2O_4$  and Aerozine 50.

The thrust chamber tests of the quartz domes were successful. Neither dome showed evidence of failure of the quartz material or of the dome sealing arrangement. Also, other development tests were conducted in an oven to verify the dome design. Both types of tests are summarized in Table 1.

I, C, Summary (cont.)

The final optical and mechanical designs for the experimental periscope have been completed.

II. TECHNICAL EFFORT

A. QUARTZ DOME DEVELOPMENT

Effective protection and cooling of the optical system has been of primary concern since the outset of the periscope development program. Several materials were investigated to find one with the physical properties needed for an optical heat shield. These materials included sapphire, magnesium oxide, and fused quartz.

The use of sapphire was considered because of its high melting point ( $3,682^{\circ}\text{F}$ ). However, it is expensive and difficult to grind (it is often used as an abrasive). Another disadvantage of sapphire is that it conducts heat from the combustion zone to the optical elements at a much higher rate than quartz. Its thermal conductivity is  $14.6 \text{ Btu/ft-hr-}^{\circ}\text{F}$ , compared with a thermal conductivity of  $0.68 \text{ Btu/ft-hr-}^{\circ}\text{F}$  for quartz.

II, A, Quartz Dome Development (cont.)

Magnesium oxide also was considered for use as a heat shield. This material has a very high melting point, but is also difficult to grind and polish. The thermal conductivity of magnesium oxide is also greater than quartz, 14.6 Btu/ft-hr-°F, compared with 0.68 Btu/ft-hr-°F. Its cost is considerably greater than either sapphire or fused quartz, particularly in sizes large enough for the periscope design. Therefore, fused quartz was selected as the most practical material to be ground to the desired hemispherical shape to protect the optical elements of the periscope. Also, heat transfer analyses (Appendix) further verified the practicality of quartz as the dome material.

Three fused quartz blanks were cut and ground to an inside spherical radius of 0.625 in. and a thickness of 0.25 in. The hemispherical domes were fine-ground to the required tolerances and mounted on stainless steel base plates that were machined to the shape of the periscope housing. The grinding process results in a dome that is opaque and not of optical quality. The domes were squarely cut at their base.

II, A, Quartz Dome Development (cont.)

Two methods of sealing the dome to the base plate were selected. These two sealing methods were evaluated on the first two quartz dome test fixtures by thermal analysis.

One dome was installed in a test fixture with high-temperature resin between the base of the dome and the test fixture base plate. This dome sealing arrangement was evaluated in an oven test in which the fixture was heated to 500°F. During the oven test, the dome cracked around its base because of different coefficients of thermal expansion between the quartz and the cement. These differences resulted in thermal stresses that caused the quartz, a relatively fragile material, to crack.

In a second quartz dome sealing design, an Invar expansion ring was used to relieve stresses in the quartz as the test fixture was oven-heated to 1,000°F. The inside surface of the expansion ring was bonded to the outside of the dome at its base with a high-temperature bonding agent. The expansion ring was then secured to the dome base plate at its outside diameter with the same bonding agent. This

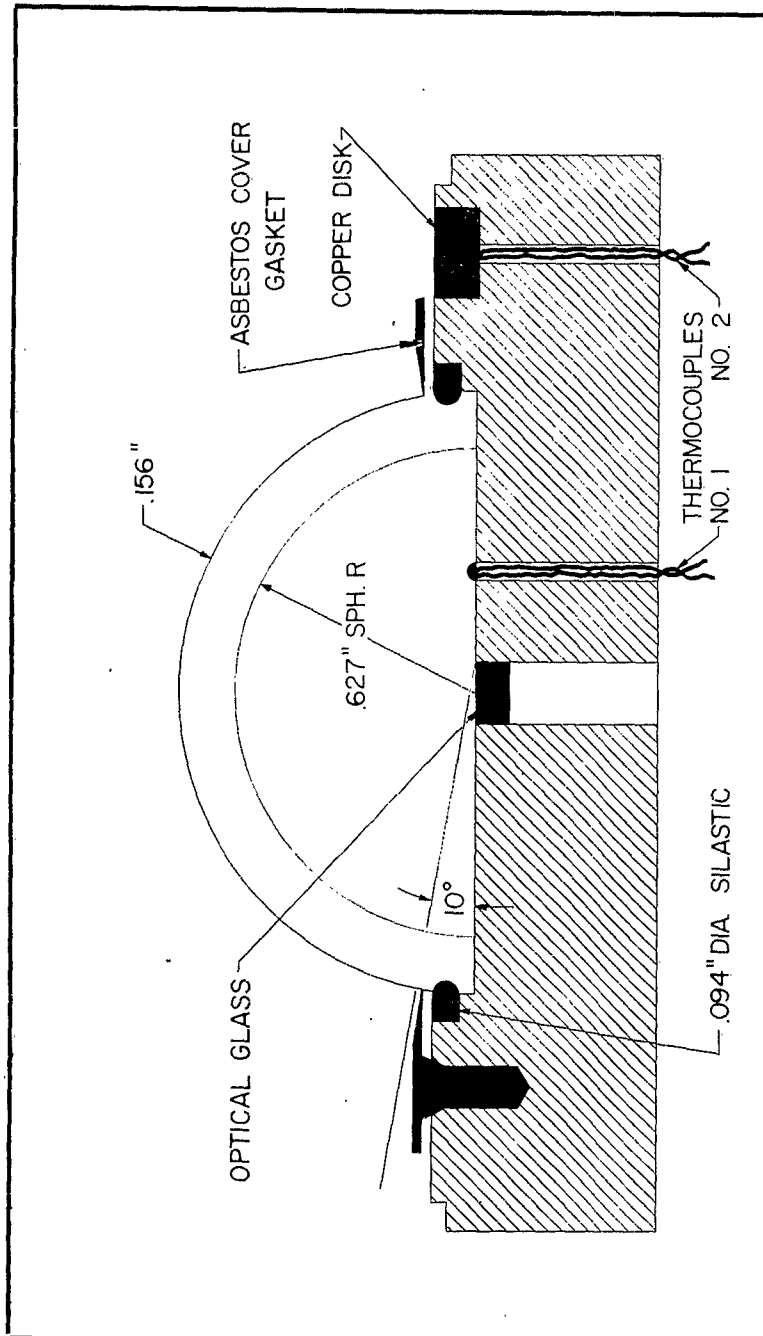


II, A, Quartz Dome Development (cont.)

dome sealing arrangement was then evaluated in an oven test identical to that used to evaluate the previously described design. The dome failed in the same manner as the previous design, i.e., a crack parallel to the base plate completely circumscribed the dome.

Because these dome sealing arrangements were not successful, two steps were taken to relieve the stresses induced in the domes. The first was to make the dome thinner. The same internal dimensions were used, but the thickness was reduced to 0.157 in. because the previous domes were believed to have failed partly because of stresses induced entirely within the relatively thick dome material. The dome sealing arrangement was also modified to permit expansion of the quartz dome at its base.

The third dome design was mounted in the manner illustrated in Figure 2. A semicircular groove was ground on the external surface of the dome near its base. A Silastic rubber O ring was placed in the



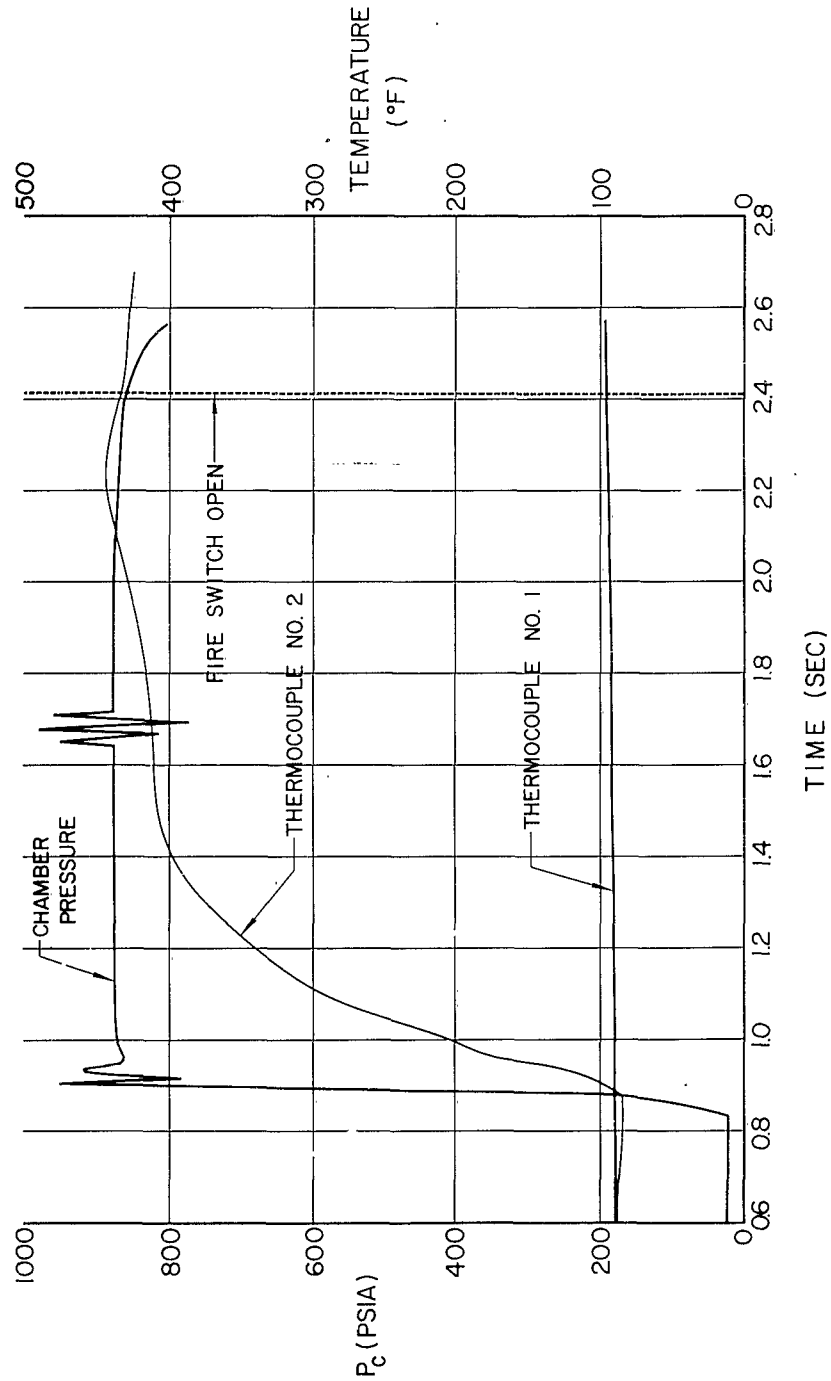
Quartz Dome Test Fixture

II, A, Quartz Dome Development (cont.)

groove in the dome and covered by an asbestos gasket to protect the rubber from the heat expected in subsequent testings. The quartz dome assembly was firmly secured to the periscope housing by machine screws and a stainless-steel ring.

To determine the heat flux to the injector face near the quartz dome, a copper disk, shown in Figure 2, was mounted in the test fixture. The disk was thermally isolated from the test fixture base plate by an epoxy compound. A thermocouple (No. 2, Figure 2) was attached to the back of the copper disk to determine the heat input rate from the combustion process.

The heat flux to the injector face was calculated from the data obtained during the thrust-chamber tests described below. Typical data are graphically shown in Figure 3. The calculations indicate that the heat flux was between 1 and 3 Btu/in.<sup>2</sup>-sec-°F. Specific values for heat flux from these tests for which valid information was obtained are as follows:



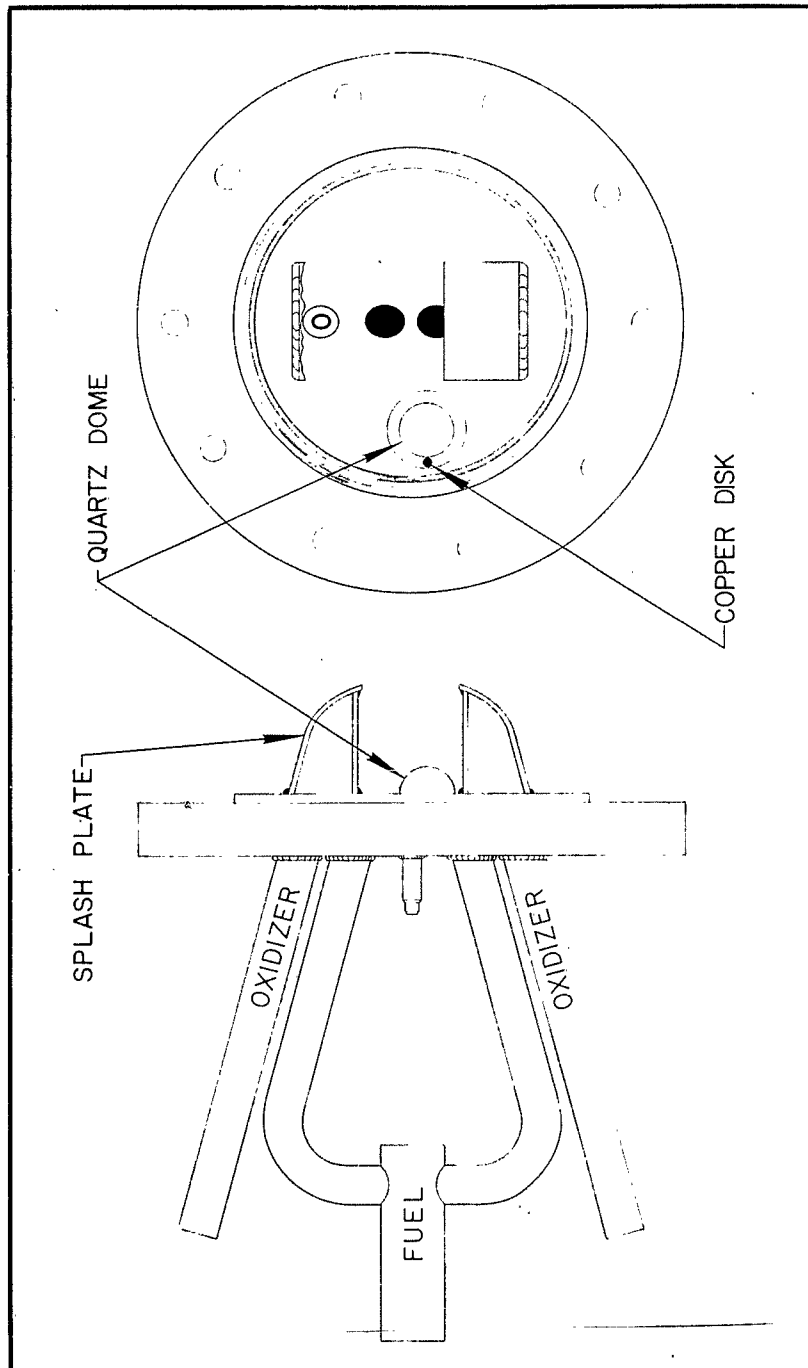
Quartz Dome Test

## II, A, Quartz Dome Development (cont.)

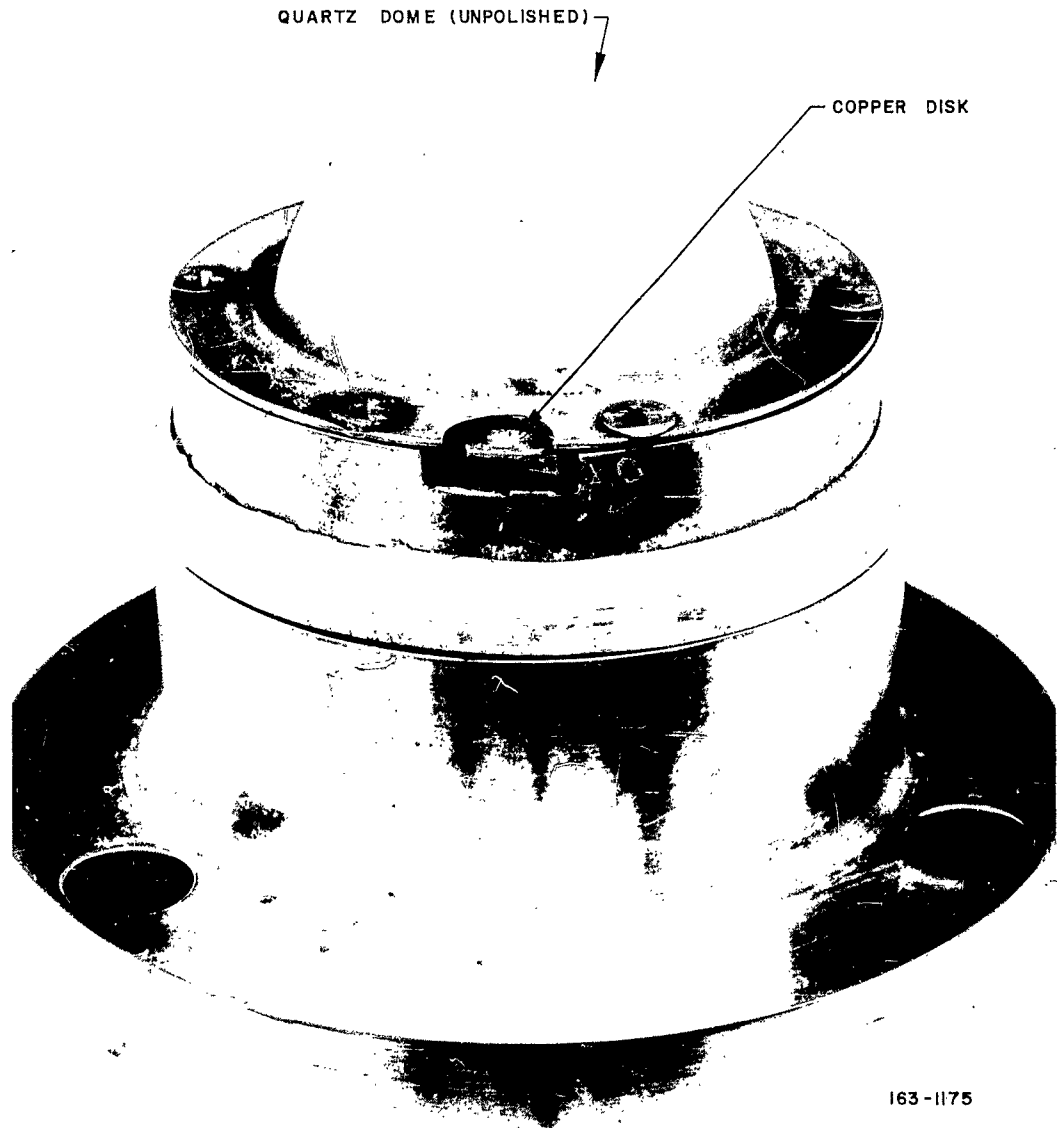
<u>Test</u>	<u>Heat Flux (Btu/in.<sup>2</sup>-sec-°F)</u>
3	1.85
4	1.27
5	2.30

These heat flux data appear to be reasonable values for the combustion-chamber region in which the calorimeter was located. Figure 4 shows the quartz dome test fixture located in the fan created by the impinging fuel streams of the single-element injector used for these tests. Therefore, this location is relatively cool and one in which the quartz dome would probably survive for a considerable length of time. As seen in Figure 3, the temperature stabilized at 450°F, the highest temperature recorded by the thermocouple throughout the test series.

The third dome, shown in Figure 5, was fine-ground but not polished to optical quality. This approach was taken to evaluate the quartz material in the desired configuration without incurring the cost of a fine optical polish. The fixture was tested in an oven



Quartz Dome Test Injector



Quartz Dome Test Fixture No. 1

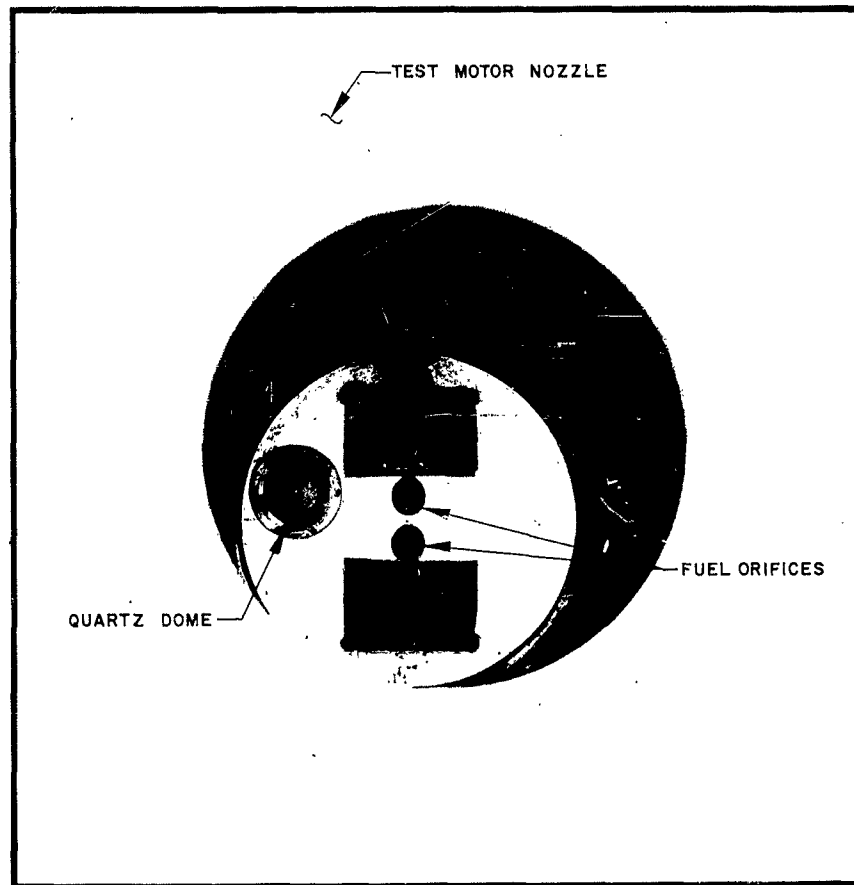
II, A, Quartz Dome Development (cont.)

preheated to 500°F. Of particular interest during this test was the ability of the dome sealing arrangement to properly provide for expansion of the quartz without inducing stresses that would fracture the material, as was previously experienced. Neither 15 minute exposure at 500°F nor subsequent cooling damaged the dome. These oven tests and the subsequent thrust-chamber tests have been summarized in Table 1.

The dome test fixture was then installed in an uncooled thrust chamber for seven tests at 850 psia chamber pressure.

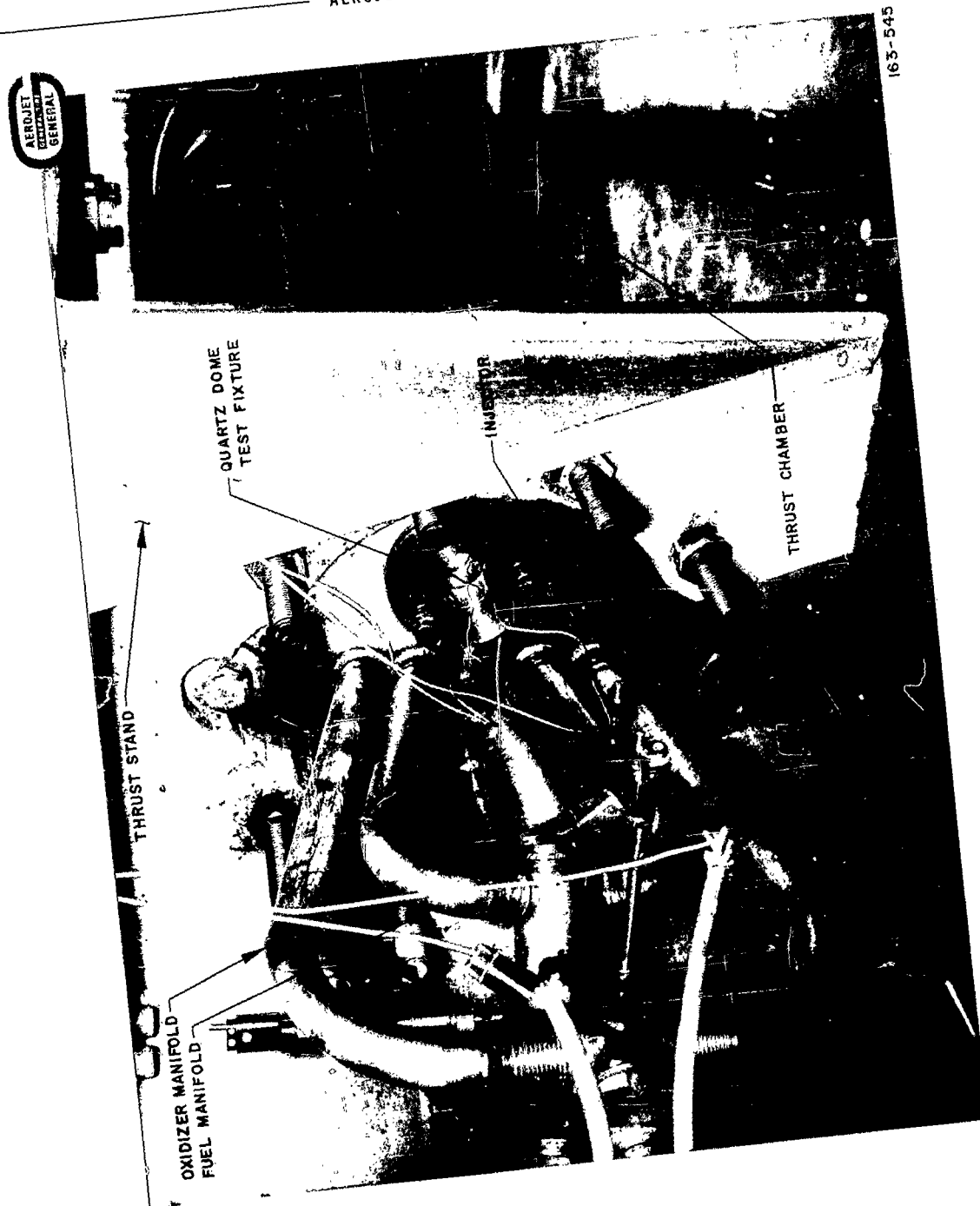
The thrust chamber assembly used for the dome tests was an experimental one previously used for injector performance investigations, and thus was available at no cost to the program. The quartz-dome test fixture was installed in the injector illustrated in Figure 4. This injector, one of the large-thrust-per-element type, was modified to provide a flush mounting of the fixture with the injector face. This installation, shown in Figures 6 and 7, would provide maximum protection for the complete optical system of the periscope. Since the injector used for these evaluation tests was operated at





163-1028

Quartz Dome Test Installation



Quartz Dome Test Motor

II, A, Quartz Dome Development (cont.)

off-design conditions (reduced flow rates, pressure drops, etc.), low-frequency instability (chugging) was present during the dome tests at 850 psia chamber pressure. This instability resulted in chamber pressure oscillations as great as 400 psi, double amplitude, at a frequency of approximately 10 cps. While these certainly were not optimum operating conditions for the injector, the operating conditions resulted in a severe test of the quartz dome and the arrangement used to seal it. The dome survived the evaluation tests without loss of optical quality and was properly sealed after the tests.

The following was tested in the quartz-dome evaluations:

(1) the quartz dome and sealing arrangement, (2) the heat resistance of the quartz to combustion gases and, (3) the ability of the dome sealing arrangement to provide for expansion of the quartz when subjected to thermal shock. All tests were conducted with the  $N_2O_4$ /Aerozine 50 propellant combination.

II, A, Quartz Dome Development (cont.)

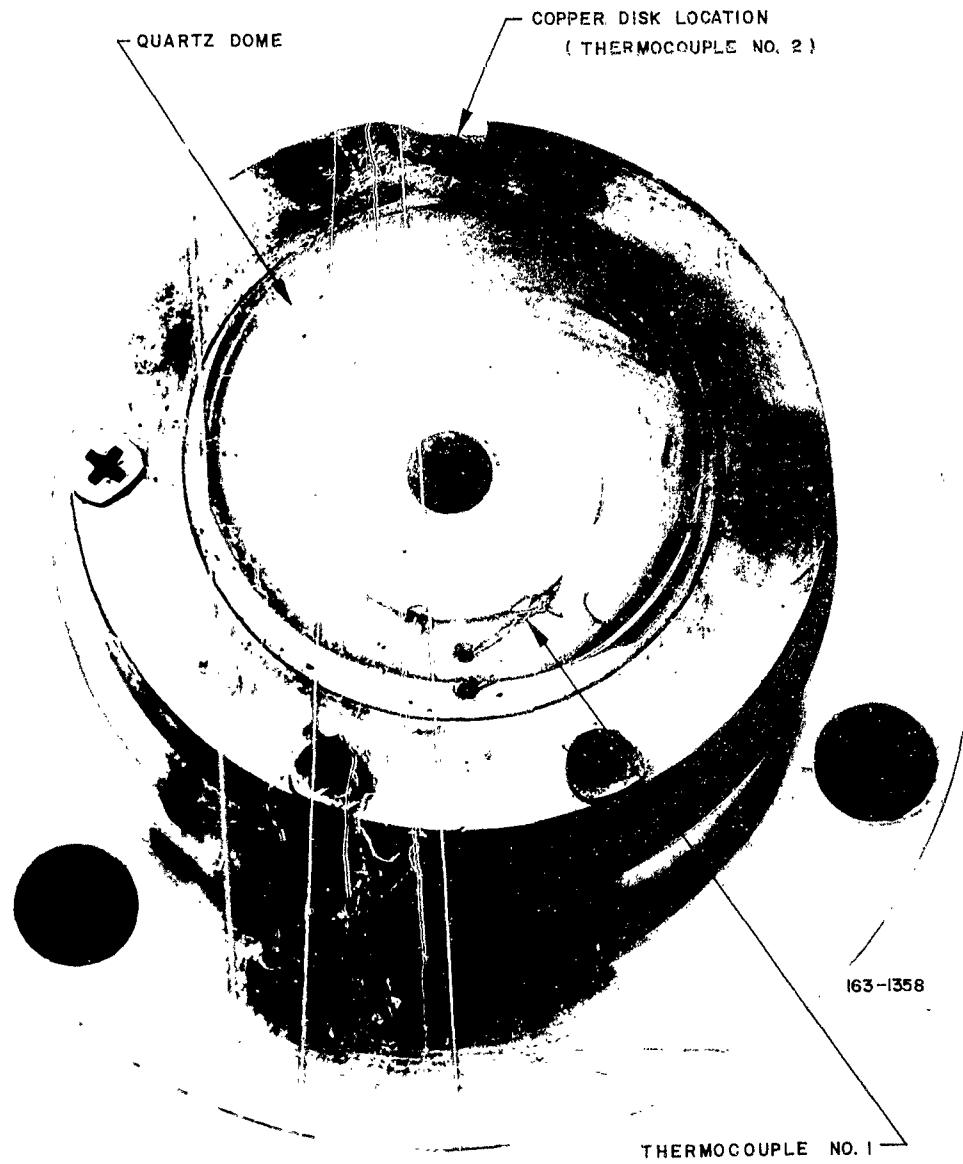
The first test series consisted of five tests, which were conducted on the fine-ground, unpolished quartz dome (Figure 5). In the first test, the chamber pressure was held to 750 psia and the mixture ratio was set at 0.95:1 so that the firing would be relatively cool. The mixture ratio was progressively increased, and a setting of 2.2 was used for the fifth test. The chamber pressure was increased to a maximum of 863 psia during the fifth test. (These operating conditions produce a theoretical combustion temperature of 5,500°F.) In the five tests, the test fixture accumulated about 6 sec exposure to combustion (at chamber pressure) without damage to the dome.

In the second series of tests (two tests), a polished, optical quality dome was used. This dome differed from the first quartz dome only with respect to the polished surface. These two tests were of 1 and 2 sec duration; both were at about 850 psia chamber pressure and at a mixture ratio of 2:1.

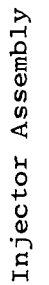
II, A, Quartz Dome Development (cont.)

After the tests, the polished surface of the quartz dome was undamaged and was of high-optical quality (Figure 8). The calorimeter was burned out of the test fixture during the last test in the series. The photograph shows the melted epoxy insulating compound splashed against the exterior surface of the dome. The residue of the epoxy resin, which was baked on the surface of the dome, was the only detrimental effect of the test. The surface of the dome was not eroded by the combustion gases, and the light transmission of the quartz was the same as before the evaluation tests. The dome appeared to be capable of withstanding the environmental conditions of these tests for several minutes without serious damage.

The periscope is designed to be placed in the center of a conventional injector, such as that illustrated in Figure 9. The quartz dome will be subjected to operating conditions somewhat different from those encountered during the dome evaluation tests, and will probably encounter a higher heat flux and equilibrium temperature in the conventional injector. However, the quartz dome is capable of withstanding an equilibrium temperature in excess of 1,000°F, whereas



Quartz Dome Test Fixture No. 2



II, A, Quartz Dome Development (cont.)

the maximum temperature observed in tests to date was less than 500°F. The central injector area may be cooled by excess fuel injection near the dome or by the introduction of gaseous nitrogen around the periphery of the dome. These measures are not expected to be needed, but they are available if extremely high dome operating temperatures are encountered.

The heat flux values observed during these tests, when related to the theoretical analysis made on the quartz material, yield some indication to the probable life of a quartz dome in the required application. Although the conclusions that can be made are not absolute, the best estimate on the life of the quartz is as follows:

Under the most negative assumptions, i.e., no heat is conducted away from the dome, either through to the area beneath the dome or across the contact area on which the dome is seated, the dome will remain effective for only 3 sec. However, the dome should survive an environment similar to that found in these tests for some period of time longer than 3 sec. Nevertheless, the combustion instability present in the chamber can almost always be visually analyzed in the initial 3 sec of testing.

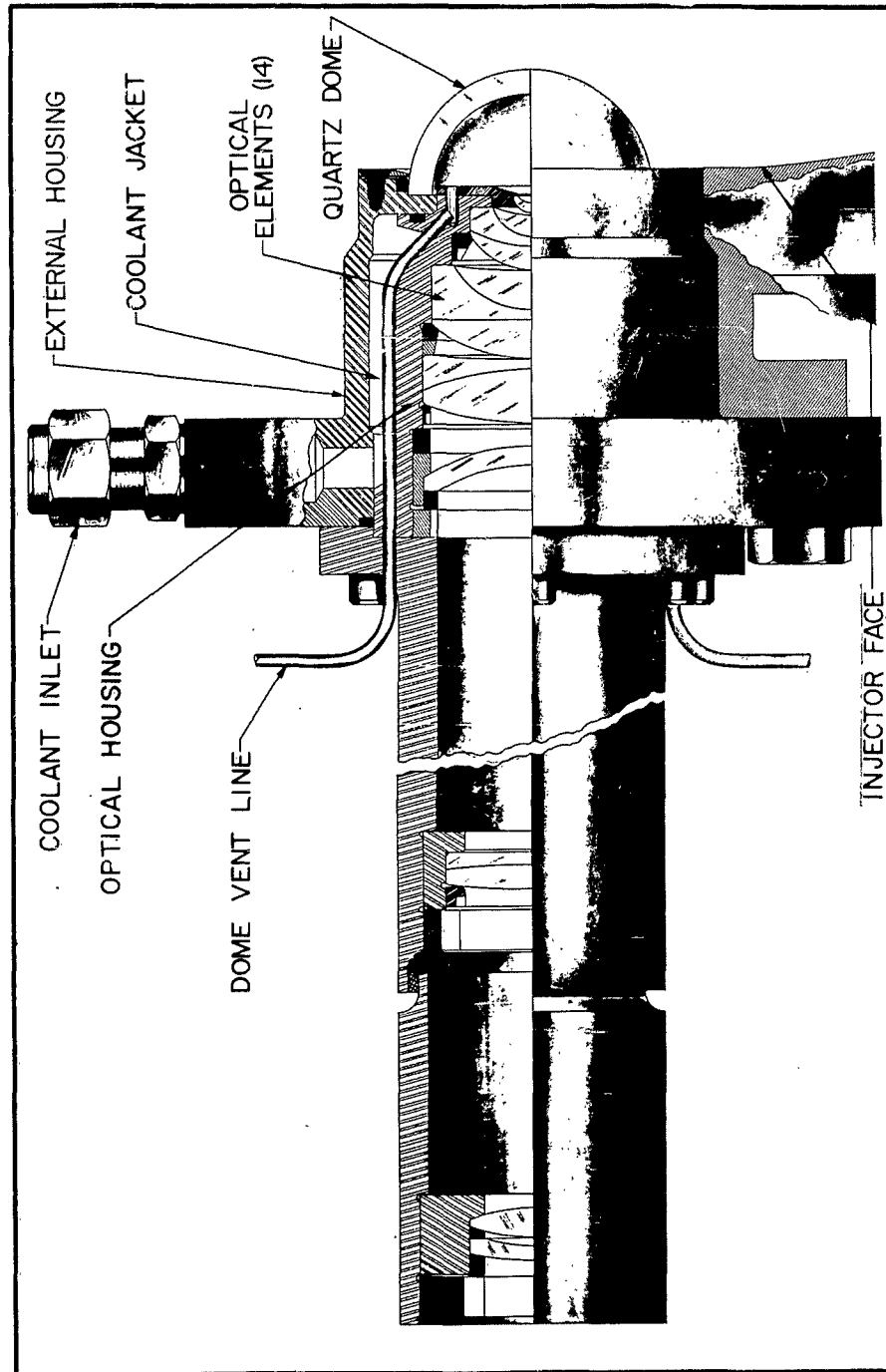


II, A, Quartz Dome Development (cont.)

B. OPTICAL DESIGN

The periscope is composed of 14 elements and produces a field of view of  $160^{\circ}$ . The circular collimated beam can be placed entirely within the rectangular format of standard 16mm motion-picture film, and a high-speed camera may be used to record high-frequency instability processes and other combustion phenomena within the chamber.

A unique feature of the optical system of the periscope (Figure 10) is the design of the objective (frontal element) lens in the optical train. The front element in an ordinary wide-angle optical system is a large, convex surface that allows the principal rays to enter the system as nearly perpendicular to the surface of the element as possible. A 2- to 3-in. diameter frontal element is ordinarily needed for optical system with a  $160^{\circ}$  field of view. However, the periscope obviates this by using a very small concave frontal element that accepts the entire light-ray envelope through a 0.1-in. diameter aperture in the plane of the injector face. The frontal element is located behind the aperture and collects the ray envelope



Detailed Design of Periscope Assembly

II, B, Optical Design (cont.)

for transmission to the succeeding lenses in the system. The primary advantage of this design is that it provides a wide-angle view through a small aperture without the use of low-melting-point optical elements that protrude into the combustion area.

The optics have been designed for a maximum relative aperture of  $f/4$ . This results in a system that is optically fast and will permit the use of high-quality, fine-resolution film even at high camera speeds. The system is designed to use the Wollensak WF-3 high-speed 16mm Fastax camera, which is capable of speeds to 7,000 frames/sec (14,000 frames/sec with the split-frame technique). The resolving power of the Fastax camera is limited to between 30 to 50 lines/mm. The resolving power of the periscope optical system exceeds that of the camera at all field-of-view angles.

The area of sharpest focus of the optical system is on the surface of an imaginary sphere with a 7-in. radius centered on the frontal element. However, the periscope depth of field is great enough to yield good imagery throughout the combustion chamber.

II, B, Optical Design (cont.)

There are two basic functions of the objective (frontal element) lens. First, it forms an image of the thrust chamber at the first focus surface that can be transmitted to the film plane by the relay and camera lenses. Second, the objective lens forms an image of the entrance pupil at the selected aperture stop. In this case, the aperture stop, which limits the  $f$ 'number of the periscope, is placed at the first surface of the camera lens, and the entrance pupil is located at the center of the dome. The spherical aberration of the principal rays is considerably reduced by the use of an aspheric pupil corrector, which is located near the focal surface of the objective lens.

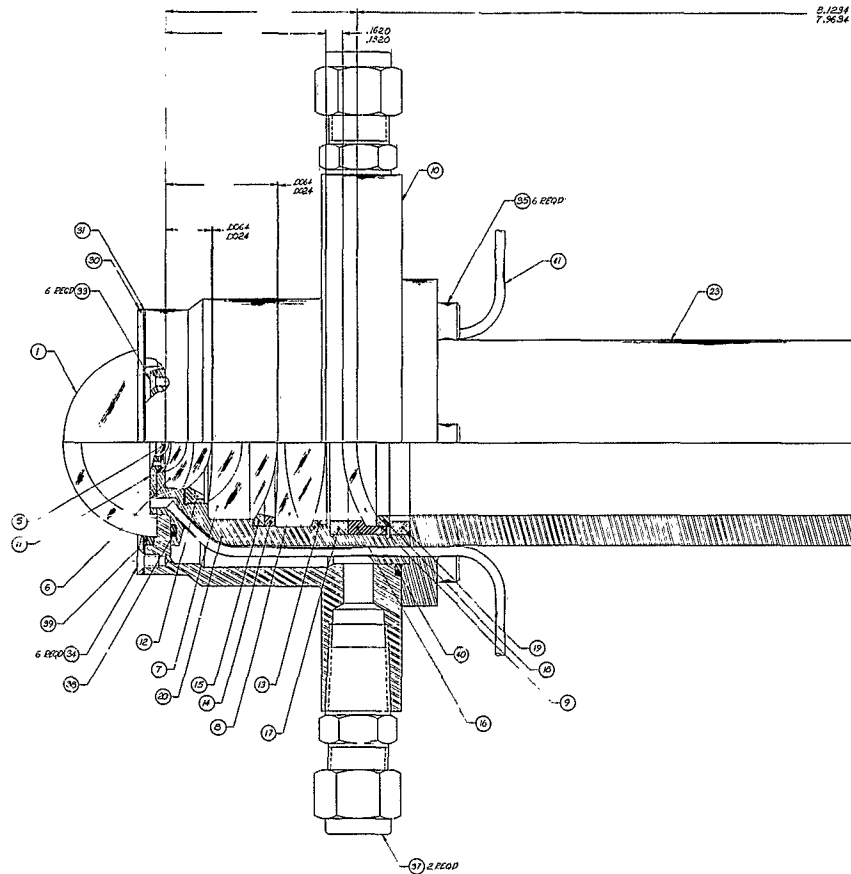
The purpose of the relay lens is to collimate the optical path between the relay lens and camera lens. Corrections for coma and astigmatism into the camera and relay lenses had to be designed to compensate for residual aberrations in the wide-angle objective lens. With the use of several elements of high-index glass, the objective lens for lateral color (variation of magnification with wave length), zonal lateral color, spherical aberration, and distortion was corrected

II, B, Optical Design (cont.)

but the aberrations of coma and astigmatism could not be completely controlled without a degree of freedom available in the camera lens design. Therefore, the periscope system contains all the optical elements needed for proper light-beam focus on the film plane. The periscope specifications appear in Table 2, and a detailed drawing of the system is shown in Figure 11.

C. MECHANICAL DESIGN

The periscope housing is constructed entirely of stainless steel. The lenses are accurately located in the housing by spacers and threaded retaining rings, all machined to very close tolerances. The periscope assembly will weigh approximately 25 lb, excluding the camera. It is 2-3/8 in. at the largest diameter (this portion of the periscope is within the injector) and 1-3/4-in. at its smallest diameter (where it emerges from the back of the injector). The assembly, without the camera, is about 14 in. long.



Page 30

Figure 11



II, C, Mechanical Design (cont.)

The periscope mounting flange contains a coolant jacket through which water, gaseous nitrogen, or liquid nitrogen may be introduced to cool the optical system. The tests conducted on the quartz dome indicate that a cooling system will not be required. The periscope design has provisions for cooling if optical investigations at high temperatures are desired.

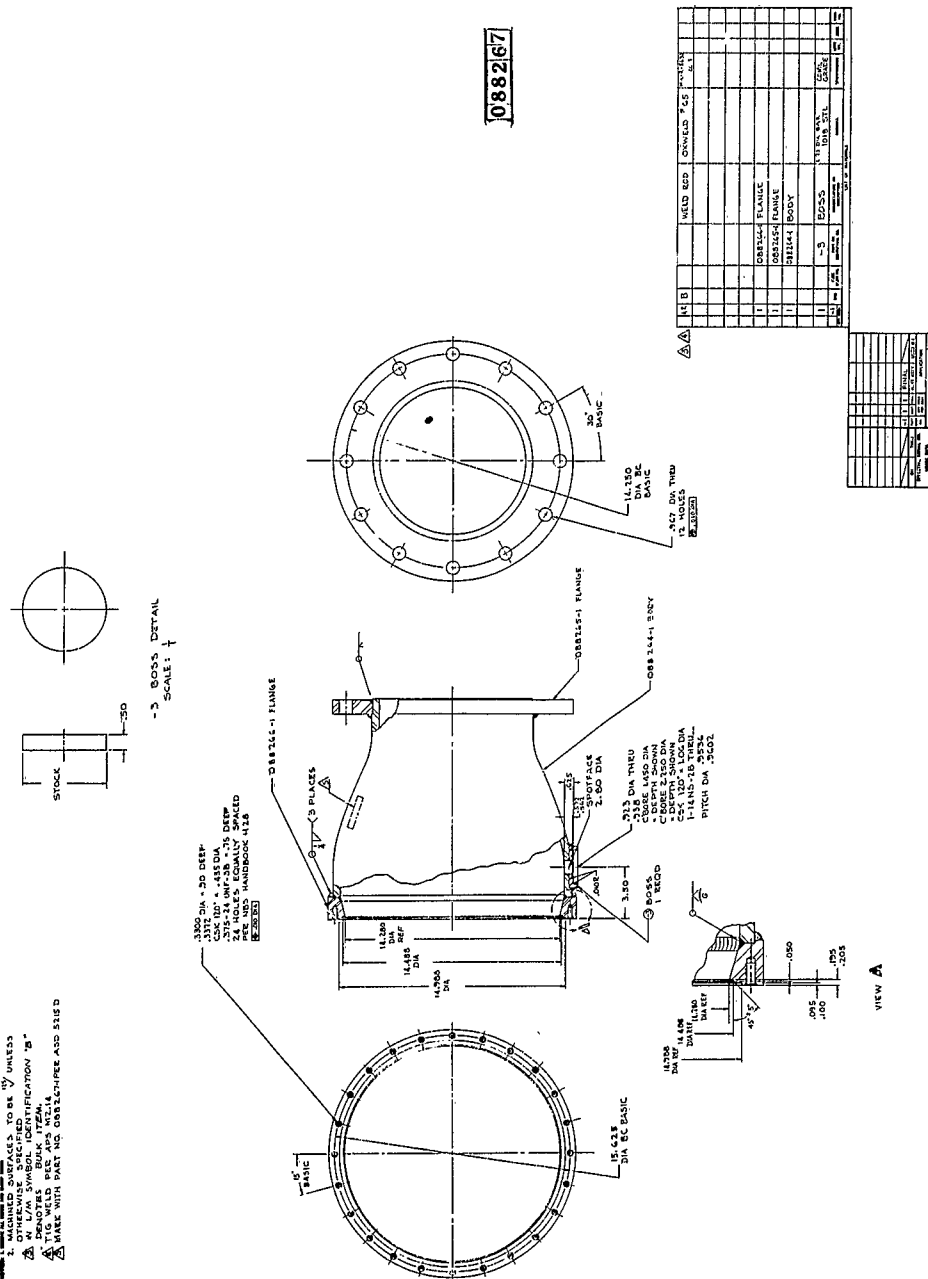
D. COMPLETED EQUIPMENT

Two major items of test hardware, an uncooled thrust chamber and an LR91-AJ-3 injector (which was modified to accept the periscope), were constructed for the periscope development program.

The uncooled chamber (Figure 12) was constructed to conduct the initial short-duration tests of the experimental periscope in the LR91-AJ-3 injector. This equipment will permit tests to 5 sec duration. The installation of a pulse-gun ring will allow the chamber to be used to determine the ability of the periscope to observe the generation of artificial shock waves during engine operation. The chamber is complete and available for immediate use.



088267



Thrust Chamber Assembly

II, D, Completed Equipment (cont.)

The LR91-AJ-3 injector to be used for experimental periscope evaluation is partially complete. The central injector area has been modified to accept the periscope and the required modifications to the propellant manifolds have been completed. The remaining work to be accomplished consists of the installation of the injector face plates and the pattern-drilling operation. The injector (Figure 9) is now in storage and is available for future use.

The grinding laps and test plates to be used in the construction of the optical system of the periscope have been manufactured. These items are needed to grind and polish the individual optical elements of the system to the precise contour needed for proper optical performance.

E. PLANS FOR FUTURE WORK

Several years experience conducting combustion studies with pulse motors has shown that many forms of combustion instability are clearly visible.

II, E, Plans for Future Work (cont.)

High-speed photography of the combustion process through the plastic slit window of the pulse motor reveal that clearly defined, high-frequency shock waves are present during unstable combustion. However, the view of these shock waves is severely limited by the very narrow ( $1/4$ - or  $1/2$ -in.) view afforded by the slit window. Whether or not the shock waves are tangential or transverse or whether a longitudinal mode is present cannot be definitely determined by viewing the combustion process through the slit window.

The optical system of the periscope will provide a view of the entire combustion area so that the specific mode of instability may be analyzed. The completed periscope will be used in a variety of tests, the first of which will be to determine its ability to discern the various phenomenon of the combustion process. The initial tests will consist of a photographic analysis of the characteristics of pulse charges as they are used to initiate instability in standard pulse motors. This will be done with the periscope mounted in a pulse motor that is pressurized with an inert gas. The tests will be used to

II, E, Plans for Future Work (cont.)

calibrate the optical system of the periscope and to observe the precise nature of the shock waves generated by the pulse charges. Artificial illumination will be used to obtain an image during these inert-gas pulse-motor tests.

The succeeding test series will consist of hot firings with the pulse motor to observe the photographic results obtained with the periscope during the initiation of unstable combustion. The unstable combustion will be initiated by the same type of pulse charges previously photographed with the periscope during the inert-gas motor tests. High-response instrumentation will be used to compare the information obtained by using the periscope with that obtained by viewing the combustion process and the instability through the standard pulse motor slit windows.

The periscope will then be used to observe the combustion characteristics of the conventional Titan LR91-AJ-3 injector. This injector, modified for low-thrust-level operation, will be used in conjunction with an uncooled thrust chamber for tests up to 5 sec.

II, E, Plans for Future Work (cont.)

In this test series, a pulse-gun ring will be used between the injector and chamber. Unstable combustion can be initiated in this manner so that the mode of instability present in the conventional injector may be closely observed by the periscope.

The optical system of the periscope, with its wide field of view, could be used to an advantage in several locations in the combustion chamber. Placed in the wall of the thrust chamber, the periscope would be capable of observing the face of the injector to determine the characteristics of various injector patterns as well as the phenomena of propellant mixing and combustion. This location would also permit observation of the performance of devices such as baffles during combustion. Readjustment of some of the elements of the optical system will permit the use of a flat protective device (rather than the quartz dome used in this design) if a flush-mounted system is needed for a particular investigation. The periscope system is quite versatile and could be used in a variety of locations for analysis of various aspects of the combustion process.

## AEROJET-GENERAL CORPORATION

TABLE 1

## QUARTZ DOME EVALUATION TESTS

<u>Test</u>	<u>Duration*</u>	Max Temp. (°F)	P <sub>c</sub> (psia)	<u>MR</u>	<u>Results</u>
Oven	15 min	500	--	--	Failure; quartz cracked when elevated to temperature.
Oven	15 min	500	--	--	Failure; quartz cracked during re- turn to ambient temperature.
Oven	15 min	500	--	--	Successful.
Thrust chamber	1.20 sec	247	831	0.92:1	Successful; test fixture No. 1.
Thrust chamber	1.21 sec	165	785	1.76:1	Successful, test fixture No. 1
Thrust chamber	1.97 sec	278	849	2.00:1	Successful; test fixture No. 1.
Thrust chamber	2.41 sec	434	863	2.07:1	Successful; test fixture No. 1.
Thrust chamber	2.48 sec	--	863	2.09:1	Successful; test fixture No. 1.
Thrust chamber	1.57 sec	--	806	2.01:1	Successful; test fixture No. 2.
Thrust chamber	3.15 sec	--	847	1.95:1	Successful; test fixture No. 2.

\* This is actual test duration for the time elapsed between the opening and closing of fire switch. The duration noted is slightly longer than the time the fixture was exposed to chamber pressure.

Table 1

Report No. 652/SA4-2.2-F-1, Volume 6

AEROJET-GENERAL CORPORATION

TABLE 2

PERISCOPE SPECIFICATIONS

Field of view, degrees	160
Relative aperture	f/4
Effective focal length, in.	.098
Focal distance, in.	7
Shape of object field	spherical
Image format	16mm
Length of periscope, in.	14
Outside diameter, in.	1.65
Total weight of periscope, lb	25
Dome working pressure, psia	1,000
Resolution	

<u>Field of View (degrees)</u>	<u>Lines per Millimeter</u>
0	200
+50	100
+60	110
+70	116
+80	57

Table 2

Report No. 652/SA4-2.2-F-1, Volume 6, Appendix

AEROJET-GENERAL CORPORATION

APPENDIX

THEORETICAL HEAT TRANSFER TO PERISCOPE DOME



Report No. 652/SA4-2.2-F-1, Volume 6, Appendix

AEROJET-GENERAL CORPORATION

FIGURE LIST

	<u>FIGURE NO.</u>
Dome Temperature History (Isolated Dome)	1
Temperature History (Dome Apex)	2

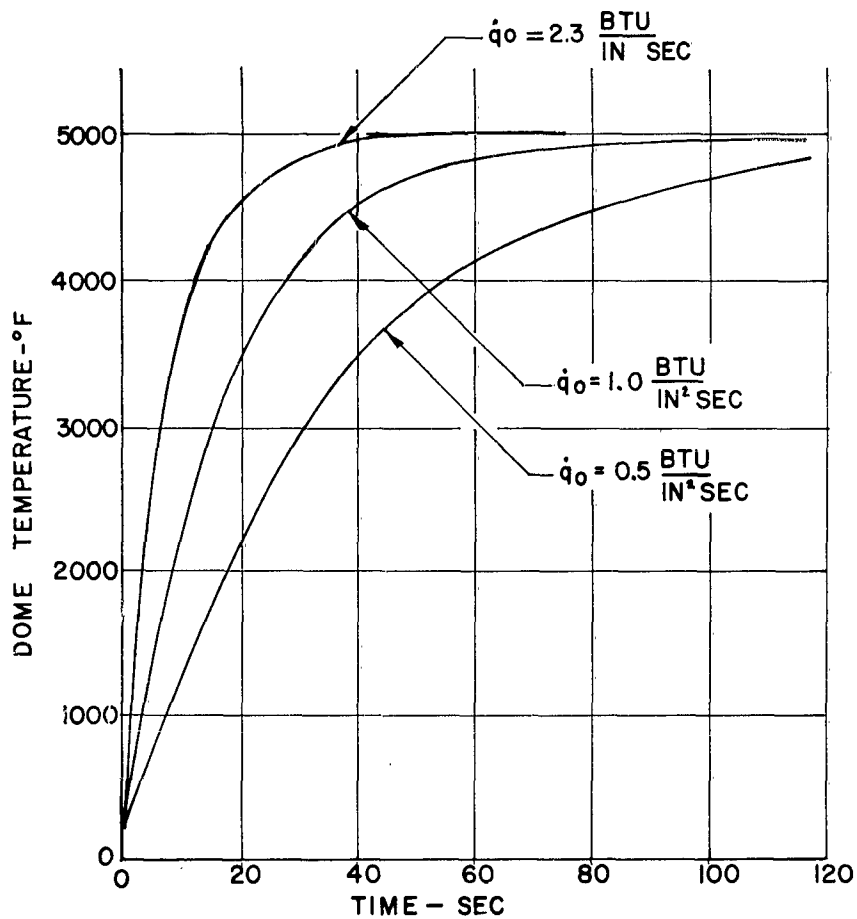
I. MAXIMUM DOME TEMPERATURE

Before the design of the quartz dome was finalized, theoretical studies were performed to determine maximum dome temperatures. The equation for the temperature history of the dome is:\*

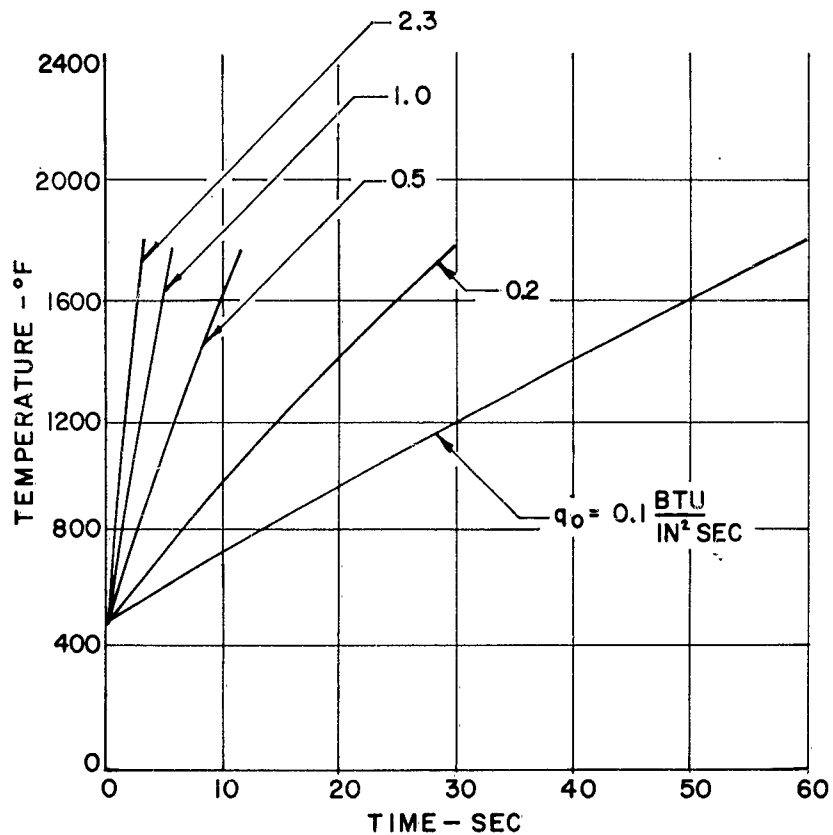
$$T - T_o = \frac{hA}{hA + U} (T_g - T_o) \left[ 1 - e^{-\left(\frac{hA}{mc} + \frac{U}{mc}\right)t} \right]$$

The derivation of this formula is given below. Figure A1 shows the temperature of the dome versus time for three heat fluxes, assuming a thermally isolated dome (i.e.,  $U = 0$ ). Figure A2 shows the dome apex temperature versus time for several heat fluxes. These calculations were based on the assumption of a constant temperature over the entire outer surface. The analysis is of value when experimental data for the temperature and heat flux are found for three points: the apex of the quartz dome, the base of the dome, and the injector face. In practice it was only possible to measure the temperature and heat flux at one point (the injector face). Therefore, the life of the dome cannot be positively determined. The dome, in an environment similar to that in the test motor, will survive for

\* Symbols are defined at end of appendix



Dome Temperature History (Isolated Dome)



Temperature History (Dome Apex)

I, Maximum Dome Temperature (cont.)

at least 3 sec. Although the dome will probably survive considerable longer than that, the extent of the life depends on the specific temperature encountered by the dome apex. The maximum temperature of the dome will also depend on the environment generated by the injector under study. The difficulty in determining the temperature encountered by the dome is due to the boundary layer of cooler gas, which exists on the dome surface and cannot be accurately defined. Since the boundary layer of gas does exist, however, its effect will be to cool the dome. The quartz dome has a finite conductance, however small, and its effect will again be to cool the dome. Therefore, the theoretical temperature histories described by Figures A1 and A2 represent conservative estimates of conditions the dome will encounter.

II. DOME-TEMPERATURE EQUATION

The equation for the temperature history of the dome is derived below:

II, Dome-Temperature Equation (cont.)

The heat balance for the dome is:

$$hA (T_g - T) - U (T - T_o) = mc \frac{dT}{dt} \quad (\text{Eq 1})$$

Solving for dt,

$$dt = \frac{d(T - T_o)}{\frac{hA}{mc} (T_g - T) - \frac{U}{mc} (T - T_o)} \quad (\text{Eq 2})$$

Equation 2 is reduced by subtracting  $\frac{hA}{mc} T_o$  from the first term in the denominator and adding it to the second term.

$$dt = \frac{d(T - T_o)}{\frac{hA}{mc} (T_g - T_o) - \left(\frac{hA}{mc} + \frac{U}{mc}\right) (T - T_o)} \quad (\text{Eq 3})$$

Integrating

$$t = \frac{-1}{\left(\frac{hA}{mc} + \frac{U}{mc}\right)} \ln \left[ \frac{hA}{mc} (T_g - T_o) - \left(\frac{hA}{mc} + \frac{U}{mc}\right) (T - T_o) \right] + C \quad (\text{Eq 4})$$

The integration constant, C, is determined

$$T = T_o \text{ at } t = 0, \text{ therefore } C = \frac{1}{\left(\frac{hA}{mc} + \frac{U}{mc}\right)} \ln \left[ \frac{hA}{mc} (T_g - T_o) \right]$$

II, Dome-Temperature Equation (cont.)

Substituting for C

$$-\left(\frac{hA}{mc} + \frac{U}{mc}\right) t = \ln \left[ \frac{hA}{mc} (T_g - T_o) \left( \frac{hA}{mc} + \frac{U}{mc} \right) (T - T_o) \right] = \ln \left[ \frac{hA}{mc} (T_g - T_o) \right] \quad (\text{Eq 5})$$

Equation 5 is reduced to

$$T - T_o = \frac{hA}{hA + U} (T_g - T_o) \left[ 1 - e^{-\left(\frac{hA}{mc} + \frac{U}{mc}\right) t} \right] \quad (\text{Eq 6})$$

The following values were assumed for the constants in the dome temperature-vs-time equation:

$$T_o = 100^{\circ}\text{F}$$

$$R = 0.75 \text{ in.}$$

$$\theta_o = 45^{\circ}$$

$$A = 2\pi R^2 (1 - \cos \theta_o) = 1.035 \text{ in.}^2$$

$$q_o = 1.0 \text{ and } 0.5 \text{ Btu/in.}^2\text{-sec-}^{\circ}\text{F}$$

$$T_g = 5,000^{\circ}\text{F}$$

$$h = \frac{q_o}{(T_g - T_o)} = 0.0002041 \text{ and } 0.0001020 \text{ Btu/in.}^2\text{-sec-}^{\circ}\text{F}$$

$$\rho = 0.079 \text{ lbm/in.}^3$$

$$\delta = 0.25 \text{ in.}$$

II, Dome Temperature Equation (cont.)

$$m = \int A \delta = 0.02045 \text{ lbm}$$

$$c = 0.185 \text{ But/lbm-}^{\circ}\text{F}$$

$$\frac{hA}{mc} = 0.0558 \text{ and } 0.0279 \text{ sec}^{-1}$$

For  $U = 0$ :

$$T - T_o = (T_g - T_o) \left( 1 - e^{-\frac{hA}{mc} t} \right)$$

III. LIST OF SYMBOLS

$A$  = Surface area of dome

$c$  = Specific heat of dome

$C$  = Integration constant

$h$  = Convection heat transfer coefficient

$m$  = Mass of dome

$q_o$  = Initial heat flux to dome

$R$  = Radius of dome

$t$  = Time

$T$  = Temperature of dome

$T_g$  = Temperature of gas



III, List of Symbols (cont.)

$T_o$  = Initial temperature of dome

$U$  = Thermal conductance

$\delta$  = Thickness of dome

$\theta_o$  = Angle defining dome size

$\rho$  = Density of dome